Journal of Hepatocellular Carcinoma

Dovepress
Taylor & Francis Group

Open Access Full Text Article

ORIGINAL RESEARCH

Comparing Minimally Invasive Puncture Under Local Anesthesia to Open Laparotomy Under General Anesthesia for Establishing a Rabbit VX2 Liver Tumor Model

Gang Yuan[1,*], Ran Cui[2,*], Yanneng Xu[1,*], Jianming Luo[1], Bo Zheng[1], Wei Hu[1], Xun Zhang[1], Guangyan Si[1]

[1]Department of Interventional & Vascular, Affiliated Traditional Chinese Medicine Hospital of Southwest Medical University, Luzhou, Sichuan, People's Republic of China; [2]Department of Respiratory Medicine, The First People's Hospital of Neijiang, Neijiang, Sichuan, People's Republic of China

*These authors contributed equally to this work

Correspondence: Guangyan Si, Department of Interventional & Vascular, Affiliated Traditional Chinese Medicine Hospital of Southwest Medical University, Luzhou, Sichuan, 646000, People's Republic of China, Email Siguangyan@swmu.edu.cn

Purpose: To compare ultrasound-guided percutaneous puncture under local anesthesia (LA) versus open laparotomy under general anesthesia (GA) for establishing a rabbit VX2 liver tumor model, evaluating efficacy, safety, animal welfare, and tumor biology.

Methods: Twenty-eight rabbits were randomly assigned to Group A (ultrasound-guided percutaneous under LA, n = 14) or Group B (open surgery under GA, n = 14). Parameters compared included anesthesia and operation time, intraoperative blood loss, surgical trauma, postoperative complications, mortality, tumor implantation success rate, tumor volume, and tumor characteristics were evaluated via imaging and histopathological analysis.

Results: Compared to Group B, Group A demonstrated significantly shorter anesthesia preparation time (61.00 ± 6.70 s vs 632.60 ± 67.84 s, $P < 0.0001$) and operation time (4.99 ± 0.65 min vs 28.57 ± 5.35 min, $P < 0.0001$), alongside significantly reduced intraoperative blood loss (0.75 ± 0.26 mL vs 3.96 ± 0.77 mL, $P < 0.0001$). No significant differences were found in tumor implantation success rate (92.9% vs 85.7%) or tumor volume between the groups. However, Group A showed significantly lower rates of peritoneal seeding (7.1% vs 42.9%, $P = 0.037$) and abdominal wall invasion (0% vs 35.7%, $P = 0.045$). Group A also exhibited favorable trends in postoperative infection and mortality rates.

Conclusion: Ultrasound-guided percutaneous puncture under LA is a superior method for creating the VX2 liver model. It is faster, less invasive, reduces bleeding and tumor dissemination risk, maintains equivalent tumorigenicity, and better adheres to animal welfare principles.

Keywords: VX2 liver tumor model, minimally invasive puncture, local anesthesia, open laparotomy, comparative study

Introduction

Hepatocellular carcinoma (HCC) is a malignant tumor with high global incidence and mortality rates, characterized by complex pathogenesis and significant therapeutic challenges.[1] The development of animal models that accurately recapitulate the pathophysiological features of human HCC is fundamental for investigating its mechanisms and evaluating novel treatment strategies. Among various preclinical models, the rabbit VX2 liver tumor model has emerged as one of the most valuable tools for interventional therapy, imaging evaluation, and combined local-systemic treatment studies of liver cancer, owing to its hypervascular nature, rapid growth cycle, and anatomical suitability for interventional procedures, features that closely resemble human HCC.[2–4] Established via orthotopic transplantation of tumor tissue fragments, this model effectively simulates the biological behavior of liver cancer and provides a standardized platform for validating the efficacy of local therapies such as transarterial chemoembolization (TACE) and radiofrequency ablation (RFA).[5–7]

https://doi.org/10.2147/JHC.S588361
Received: 12 December 2025
Accepted: 6 February 2026
Published: 13 February 2026

Conventional establishment of the rabbit VX2 model relies on open laparotomy under general anesthesia (GA). However, this approach has notable limitations. First, GA may induce systemic risks such as respiratory depression and hemodynamic fluctuations, while potentially compromising immune function, thereby interfering with the tumor microenvironment and the accuracy of experimental outcomes.[8] Second, open surgery is highly invasive, requiring incision of the abdominal wall and liver capsule, which not only increases the risk of postoperative complications such as adhesions and wound infections,[9–12] but also demands a high level of surgical expertise. More critically, the surgical trauma itself may activate stress and inflammatory responses, potentially promoting tumor cell shedding and dissemination, thereby altering the natural progression of metastasis and introducing confounding variables into studies.[13] Furthermore, even within the open laparotomy approach, technical variations exist that can influence outcomes, underscoring the need for technique standardization.[12]

Recent advances in minimally invasive interventional techniques have created novel opportunities for establishing this animal model. Percutaneous implantation under image guidance, such as ultrasound or computed tomography (CT), allows precise tumor targeting and transplantation while substantially minimizing surgical trauma.[14,15] Furthermore, local anesthesia (LA) combined with sedation has demonstrated both safety and efficacy in complex clinical interventional procedures,[16] supporting its rationale for translational application in animal studies. The utility of minimally invasive puncture for targeted delivery of therapeutic agents (eg, drug-eluting beads, nanoparticles) and for treatment monitoring has further driven its adoption.[17–19]

Previous comparative studies of percutaneous, image-guided implantation versus open surgical approaches have laid the groundwork for less traumatic model generation.[10,11] These investigations confirmed that percutaneous techniques performed under GA reduce surgical trauma relative to laparotomy. Building on this foundation, a critical yet underexplored question remains: can combining a percutaneous approach with LA, instead of GA, yield additional significant benefits? The use of LA avoids the systemic complexities and physiological disturbances associated with GA. Moreover, emerging evidence suggests that local anesthetics may modulate the tumor microenvironment, potentially influencing metastatic behavior.[20,21] Therefore, this study is designed as a randomized controlled trial to specifically isolate and evaluate the impact of anesthesia modality within a minimally invasive framework. We compare ultrasound-guided percutaneous puncture under LA with conventional open laparotomy under GA, assessing not only procedural efficiency but also animal welfare outcomes, complication profiles, and the preservation of core tumor biology.

Materials and Methods

Experimental Animals and Grouping

This study was approved by the Animal Care and Use Committee of Southwest Medical University (Approval No: SWMU20210409). All procedures were conducted in strict accordance with the National Standards of the People's Republic of China "Guideline for Ethical Review of Animal Welfare" (GB/T 35892-2018) and the ARRIVE 2.0 guidelines. A total of 28 specific pathogen-free (SPF) male New Zealand white rabbits aged 2−3 months were supplied by the Experimental Animal Centre of Southwest Medical University (License number: SYXK [Sichuan] 2023-0065). All rabbits were of the New Zealand White strain. Additionally, two VX2 tumor-bearing rabbits (weighing approximately 2.5 kg, with tumors carried in the gluteal muscle) were purchased from Boyue Bio-engineering Co., Ltd. (Jiyuan, China), to serve as tumor tissue donors.

The individual rabbit was the experimental unit for all analyses. The experimental rabbits were randomly assigned into two groups using a random number table: Group A (Experimental group, n = 14): Underwent ultrasound-guided percutaneous implantation of VX2 liver tumors under local anesthesia. Group B (Control group, n = 14): Underwent open surgical implantation of VX2 liver tumors under intravenous general anesthesia. All animals were housed individually under standard laboratory conditions with ad libitum access to food and water. They received daily maintenance and perioperative care from trained staff.

Harvesting and Preparation of VX2 Tumor Tissue Fragments

In strict adherence to the "Refinement" and "Reduction" principles of animal welfare, VX2 tumor tissues were harvested from donor rabbits using a minimally invasive puncture technique. The detailed procedure was as follows: Donor rabbits bearing tumors for approximately two weeks were anesthetized by intravenous injection of 3% pentobarbital sodium (30 mg/kg) via the marginal ear vein. Following satisfactory anesthesia, the rabbits were immobilized, and the Operating area was shaved and aseptically prepared. Under real-time ultrasound guidance (M7, Mindray, China), multiple tumor tissue fragments approximately 1 cm in length were percutaneously obtained from the gluteal tumor using a fully automated biopsy needle (TSK, Japan) (Figure 1A–C). After removing superficial necrotic components, the tissue fragments were immediately placed in sterile saline for subsequent use (Figure 1D). This protocol ensured the procurement of high-quality viable tissue while significantly minimizing trauma and distress to the donor animals.

Establishment of VX2 Liver Tumor Model in Recipient Rabbits

Experimental Group (Group A): Ultrasound-Guided Percutaneous Implantation Under Local Anesthesia

The procedure was performed following an optimized method established previously by our team.[22] In brief, recipient rabbits were immobilized on the surgical platform, and the upper abdominal area was shaved, disinfected, and draped. The left liver lobe was identified as the ideal implantation site under ultrasound scanning and marked on the body surface. Local infiltration anesthesia was then administered at the puncture site using 1 mL of 1% lidocaine hydrochloride injection (CSPC Pharmaceutical Group, China). Subsequently, using a specialized VX2 tumor implantation kit (comprising a 16-gauge puncture needle and a flat-tipped pusher, Figure 2A), the prepared VX2 tumor tissue fragments along with an appropriate amount of gelatin sponge, were accurately implanted into the predetermined location within the liver parenchyma under real-time ultrasound guidance (Figure 2B–D). After implantation, the puncture site was briefly compressed, and the absence of active bleeding was confirmed ultrasonically before covering the wound with a sterile dressing.

Control Group (Group B): Open Surgical Implantation Under Intravenous General Anesthesia

The procedure was performed according to a classical modeling method.[23] Briefly, recipient rabbits were anesthetized by slow intravenous injection of 3% pentobarbital sodium (30 mg/kg) via the marginal ear vein. An intravenous access (24-gauge indwelling needle) was established in the abdominal wall vein for fluid supplementation and anesthesia maintenance during surgery. After achieving satisfactory anesthesia, the rabbits were placed in a supine position, and the surgical area was routinely disinfected and draped. A vertical midline incision approximately 3─4 cm in length was made below the xiphoid process. The abdominal cavity was entered through layered dissection. The left liver lobe was gently exteriorized and protected with moist gauze. A superficial incision approximately 5 mm in depth was made on the hepatic surface using a No. 11 surgical scalpel blade. Following gentle compression for hemostasis, the VX2 tumor tissue fragments were carefully implanted into the parenchymal incision using sterile forceps. The incision was then sealed with a small piece of hemostatic sponge to prevent tissue protrusion and aid hemostasis (Figure 2E–H). After confirming the absence of active bleeding, the liver was repositioned into the abdominal cavity. The abdomen was closed in layers, and the skin incision was covered with a sterile dressing.

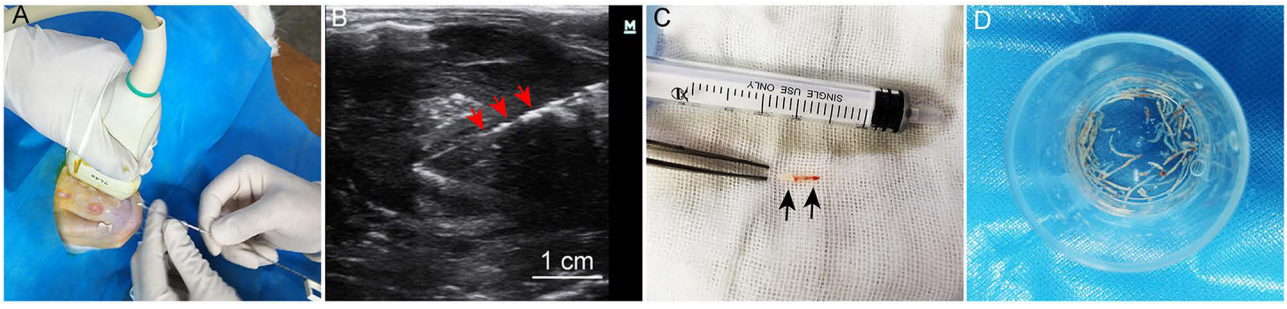

Figure 1 Harvesting and preparation of VX2 tumor tissue fragments. (**A** and **B**) Ultrasound-guided puncture of the VX2 tumor in the gluteal region of a tumor-bearing rabbit. The display screen shows the biopsy needle positioned within the tumor tissue (red arrows indicate the biopsy needle). (**C**) Intact tumor tissue fragments obtained by the biopsy needle (black arrows), approximately 1 cm in length, with minimal surface blood residue. (**D**) Tumor tissue fragments after removal of necrotic components, preserved in saline for subsequent use.

https://doi.org/10.2147/JHC.S588361

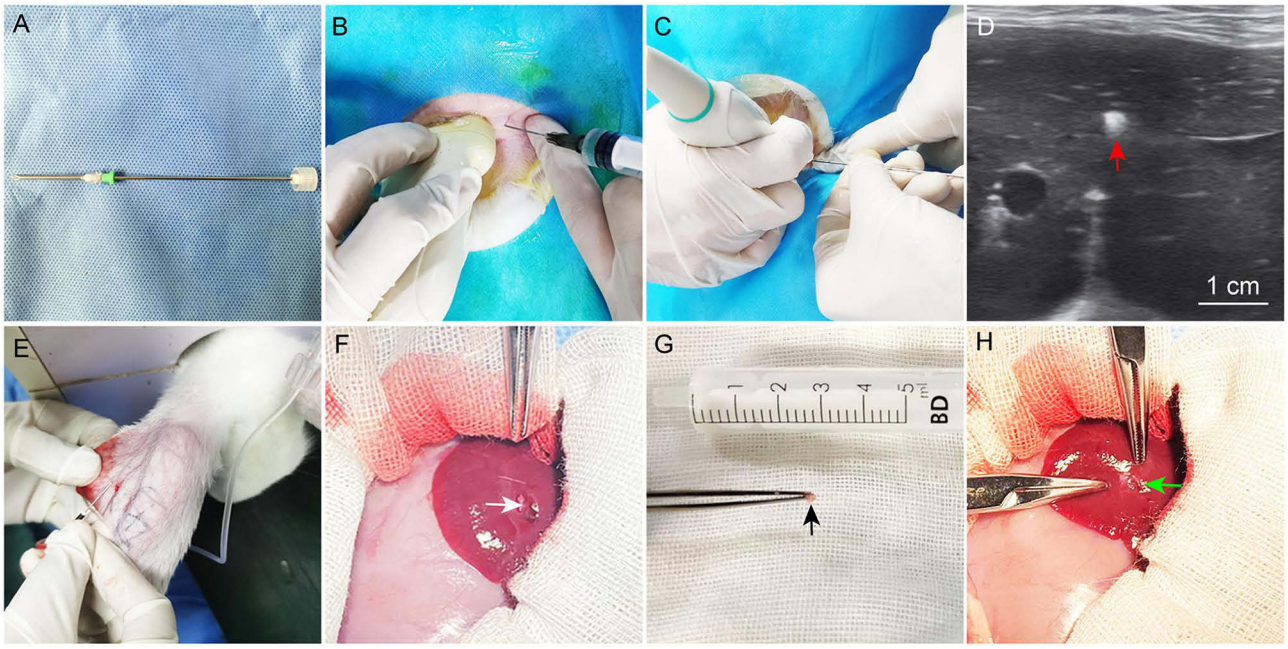

Figure 2 Implantation of VX2 tumor tissue fragments. (**A**) The VX2 tumor implantation kit comprises a smooth, flat-tipped pusher with a removable piston and a 16-gauge needle. (**B**) Ultrasound examination confirming the hepatic implantation site, followed by local infiltration anesthesia at the designated puncture point on the body surface. (**C** and **D**) Under ultrasound guidance, fresh VX2 tumor tissue fragments, along with gelatin sponge, are implanted into the liver parenchyma. Post-implantation ultrasound shows a hyperechoic gelatin sponge mass within the parenchyma (red arrow). (**E**) General anesthesia was induced by intravenous injection of 3% pentobarbital sodium (30 mg/kg) via the marginal ear vein. (**F**) After laparotomy, the liver is adequately exposed, and an implantation incision approximately 5 mm in depth is created in the parenchyma (white arrow). (**G** and **H**) Fresh VX2 tissue fragments (black arrows) are embedded into the hepatic incision and sealed with an appropriate amount of hemostatic sponge (green arrows) to achieve hemostasis.

Perioperative Management

To ensure animal welfare and control potential confounding factors, all rabbits in both groups received subcutaneous injections of meloxicam (0.1 mg/kg, for analgesia) and enrofloxacin (5 mg/kg, for anti-infection) 30 minutes preoperatively and once daily for three consecutive days postoperatively.

Imaging and Pathological Evaluation

Ultrasonography

Ultrasound screening was initiated from day 7 post-implantation, with formal evaluation conducted on day 14. All examinations were performed by a single ultrasonographer blinded to the group assignments. Tumor morphology was observed, and the longest diameter (a) and shortest diameter (b) were measured. Tumor volume was calculated using the formula V= (a × b2)/2.[24] Color Doppler flow signals were simultaneously recorded.

Contrast-Enhanced CT Scanning

Contrast-enhanced CT (CE-CT) scans were performed on day 14 post-implantation. Following anesthesia, a bolus of iodixanol (iodine 320 mg/mL, Heng Rui, China) was injected into the abdominal wall vein of the anesthetized rabbits through a 24-gauge indwelling needle at the speed of 2 mL/s, with a total amount of 5 mL. After a delay of 2 seconds, continuous scanning of the upper abdomen was initiated. Scanning parameters were set as follows: voltage 120 kV, current 80 mA, matrix 512 × 512, slice thickness 2.5 mm.

Digital Subtraction Angiography

Digital Subtraction Angiography (DSA) was performed immediately after CT scanning while the animals remained under anesthesia. The femoral artery was isolated, and a 4-French vascular sheath (Terumo, Japan) was introduced using the Seldinger technique. Under X-ray fluoroscopic guidance, a 2.4-French microcatheter (Asahi, Japan) was superselected

into the proper hepatic artery or left hepatic artery. Contrast agent was injected to perform angiography, clearly visualizing tumor-feeding arteries and tumor staining.

Pathological Examination

Upon completion of all imaging procedures, surviving animals were euthanized by an overdose of pentobarbital sodium. Liver tumors, adjacent normal liver tissue, and lung specimens were harvested in their entirety. Tissue blocks were fixed in 10% neutral buffered formaldehyde, embedded in paraffin, sectioned, and stained with hematoxylin and eosin (H&E) for observation of histological architecture and metastatic status under light microscopy.

Blinding

The ultrasonographer performing tumor volume measurements and the pathologist conducting all histopathological evaluations (including assessment of tumor characteristics, peritoneal seeding, and abdominal wall invasion) were blinded to the group allocation (A or B) of the samples. The interventional and surgical personnel performing the model establishment procedures could not be blinded due to the obvious technical differences between the approaches.

Outcome Measures and Statistical Analysis

A pre-specified analysis plan was followed. Primary outcome measures were procedural efficiency (anesthesia/operation time, intraoperative blood loss) and model success rate. Secondary outcomes included tumor volume, mortality, and complication rates (infection, peritoneal seeding, abdominal wall invasion). Given the exploratory nature of this pilot study and the limited number of pre-defined, hypothesis-driven comparisons between the two independent groups, a formal correction for multiple comparisons (eg, Bonferroni) was not applied. Such a correction was deemed overly conservative and likely to increase Type II error for this initial investigation. All P-values are reported explicitly, and findings for secondary outcomes are interpreted with appropriate caution, recognizing the need for validation in larger studies.

Statistical analyses were performed using GraphPad Prism software (version 10.1.2). Measurement data, after normality testing, are presented as the mean ± standard deviation (SD). The normality of distribution for all continuous variables was assessed using the Shapiro–Wilk test. Data conforming to a normal distribution were compared using independent samples *t*-tests. Non-normally distributed data were compared using the Mann–Whitney *U*-test. Categorical data are expressed as numbers (percentages), and between-group comparisons were analyzed using Fisher's exact test. A two-sided *P* value of less than 0.05 was considered statistically significant.

Given the exploratory nature of this pilot study and the absence of prior effect size estimates for key binary endpoints (eg, complication rates) in the specific context of LA vs GA comparison, a formal a priori sample size calculation was not performed. Instead, a sample size of n=14 per group was selected based on common practice in comparable rabbit VX2 model studies[11,12,14] and practical resource considerations. This size was anticipated to allow detection of large effects in primary continuous outcomes, such as operative time. Results, particularly for secondary binary endpoints, should be interpreted as hypothesis-generating for future adequately powered confirmatory trials.

Results

Preoperative baseline characteristics (including age, sex, and body weight) showed no statistically significant differences between the two groups ($P > 0.05$), confirming their comparability. To comprehensively evaluate the two modeling approaches, comparative analyses were conducted across several domains: anesthesia and surgical efficiency, model success rate and tumor growth, mortality, and postoperative complications.

Comparison of Anesthesia and Surgical Efficiency

As shown in Table 1, Group A demonstrated significant advantages in anesthesia and surgical efficiency. The anesthesia preparation time in Group A was markedly shorter than that in Group B (61.00 ± 6.70 s vs 632.60 ± 67.84 s, $P < 0.0001$). Postoperatively, Group A required no anesthesia recovery time, whereas Group B required an average of 58.93 ± 8.77 minutes for recovery ($P < 0.0001$). No mortality occurred during surgery or anesthesia in either group.

Table 1 Comparison of Anesthesia Differences

	LA	GA	*t* test	*p* value
No. of rabbits (n)	14	14		
Weight (kg)	2.78 ± 0.11	2.70 ± 0.10	1.95	0.0623
Anesthetic preparation time (s)	61.00 ± 6.70	632.60 ± 67.84	31.37	< 0.0001
Postoperative resuscitation time (min)	0	58.93 ± 8.77	25.15	< 0.0001
No. of mortality (n)	0	0		
Mortality rate (%)	0	0		1.00

Abbreviations: LA, local anesthesia; GA, general anesthesia.

Regarding operation performance (Table 2), the minimally invasive nature of Group A was further evidenced. The mean abdominal incision length in Group B was 3.93 ± 0.62 cm, whereas Group A exhibited only a minimal needle puncture site on the body surface. Both the operative time (4.99 ± 0.65 min vs 28.57 ± 5.35 min, $P < 0.0001$) and intraoperative blood loss (0.75 ± 0.26 mL vs 3.96 ± 0.77 mL, $P < 0.0001$) were significantly reduced in Group A compared to Group B. No mortality occurred during any surgical procedure.

Comparison of Model Success Rate, Tumor Growth, and Mortality

Model establishment was evaluated by imaging on day 14 post-operation (Figure 3). As summarized in Table 3, the tumor implantation success rate was 92.9% (13/14) in Group A and 85.7% (12/14) in Group B, with no statistically significant difference between groups ($P = 1.00$). Similarly, the tumor volumes in successfully implanted rabbits showed no significant difference (427.6 ± 73.83 mm^3 vs 483.2 ± 65.66 mm^3, $P = 0.0594$). Regarding mortality, Group A had a rate of 0% (0/14), compared with 14.3% (2/14) in Group B. Although numerically higher in Group B, this difference did not reach statistical significance ($P = 0.487$).

Comparison of Postoperative Complications

Analysis of postoperative complications (Table 4) revealed a distinct advantage for the minimally invasive Group A in controlling iatrogenic tumor dissemination. The rate of peritoneal implantation metastasis was significantly lower in Group A (7.1%, 1/14) than in Group B (42.9%, 6/14) ($P = 0.037$). Similarly, the abdominal wall invasion rate was significantly reduced in Group A (0%, 0/14) compared to Group B (35.7%, 5/14) ($P = 0.045$). Although the difference in infection rate did not reach statistical significance (0% [0/14] vs 28.6% [4/14], $P = 0.102$), Group A demonstrated a clear favorable trend.

Comparison of Welfare-Related Clinical Parameters

Clinical observations pertaining to animal welfare and stress revealed marked differences between groups. As shown in Table 1, rabbits in Group A required no recovery time from anesthesia, resuming normal posture and ambulation immediately after the procedure. In contrast, Group B exhibited a significantly prolonged recovery period, taking 58.93 ± 8.77 minutes on average to regain sternal recumbency and normal gait ($P < 0.0001$). Postoperatively, rabbits in Group A consistently resumed normal food and water intake within six hours, maintained baseline activity levels, and showed no significant weight loss over the first 48 hours. Group B, however, demonstrated notably reduced activity and food intake on the operative day, with full return to preoperative intake and activity patterns typically delayed until post-operative day 1 or 2.

Table 2 Comparison of Operation Differences

	Puncture Implantation	Laparotomy Implantation	*t* test	*p* value
Incision length (cm)	0	3.93 ± 0.62	23.87	< 0.0001
Operation time (min)	4.99 ± 0.65	28.57 ± 5.35	16.39	< 0.0001
Volume of hemorrhage (mL)	0.75 ± 0.26	3.96 ± 0.77	14.78	< 0.0001

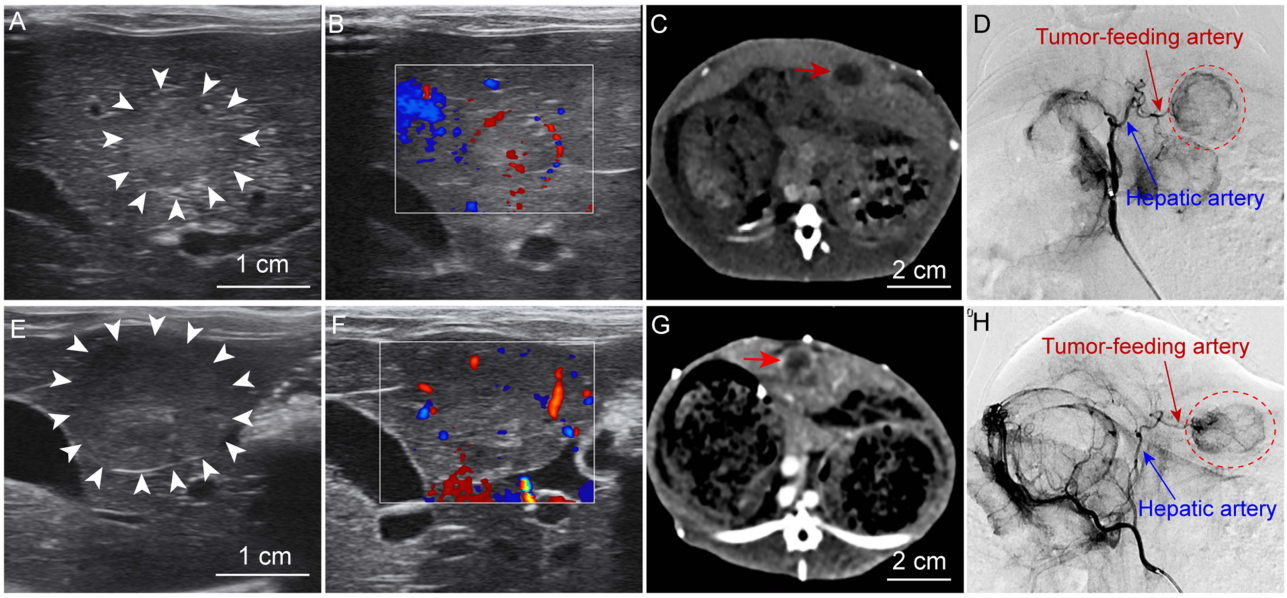

Figure 3 Imaging features of the two groups. (**A**–**D**) Puncture implantation under LA and (**E**–**H**) open laparotomy implantation under GA, imaged two weeks post-modelling. (**A** and **E**) Ultrasonography shows solitary VX2 tumors with homogeneous, slightly hypoechoic echogenicity compared to the surrounding liver parenchyma and well-defined margins (white arrows indicate tumor borders), mostly presenting as round or oval shapes. (**B** and **F**) Color Doppler reveals relatively prominent blood flow signals surrounding and within the tumors. (**C** and **G**) CE-CT demonstrates oval-shaped tumors within the liver parenchyma with clear boundaries (red arrows). (**D** and **H**) DSA shows hypervascular tumors, with clear visualization of the hepatic artery and tumor-feeding arteries (the VX2 tumor is highlighted within the red dashed circle).

Imaging and Pathological Characteristics in Both Groups

Imaging examinations (ultrasonography, CE-CT, DSA) demonstrated that the successfully established VX2 liver tumors in both groups exhibited highly similar characteristics in morphology, boundary, internal echogenicity/density, and hypervascular features (Figure 3), consistent with the typical biological profile of VX2 tumors. Pathological examination further confirmed these findings: gross specimens from both groups presented as spherical, firm masses, with cross-sections showing peripheral viable tumor tissue surrounding central necrotic areas. Microscopically, all tumors displayed

Table 3 Comparison of Tumor Formation Differences

	Puncture Implantation	Laparotomy Implantation	*t* test	*p* value
No. of rabbits (n)	14	14		–
Successfully implanted (n)	13	12		–
Successful implantation rate (%)	92.9%	85.7%		1.00
Tumor size (mm^3)	427.6 ± 73.83	483.2 ± 65.66	1.983	0.0594
No. of death	0	2		
Mortality rate (%)	0%	14.3%		0.487

Table 4 Comparison of Postoperative Complications Between Two Different Methods

Group	No. of Rabbits	No. of Infected Rabbits	Postoperative Infection Rate (%)	With Celiac Implantation	Celiac Metastasis Rate (%)	With Abdominal Wall Invasion	Abdominal Wall Invasion Rate (%)
A	14	0	0	1	7.10%	0	0
B	14	4	28.60%	6	42.90%	5	35.70%
p value			0.102		0.037		0.045

Notes: A, Puncture implantation; B, Laparotomy implantation; Fisher's Exact Test, $\alpha = 0.05$.

https://doi.org/10.2147/JHC.S588361

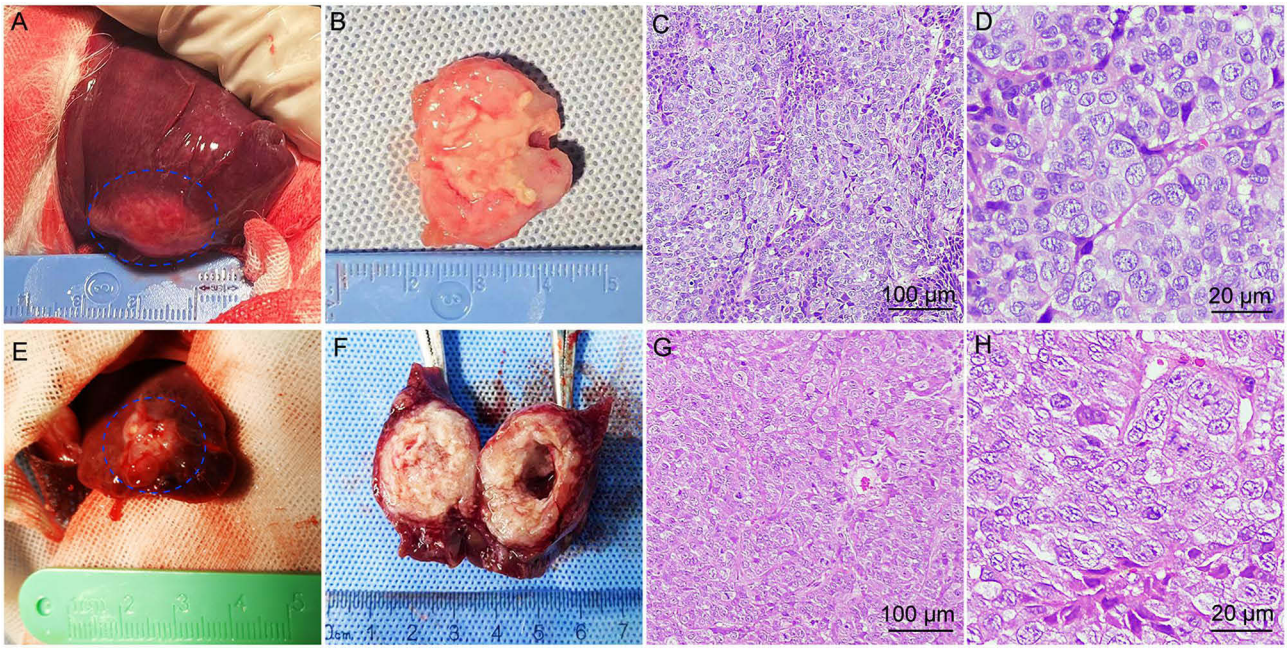

Figure 4 Pathological examination of the two groups. (**A**–**D**) Pathological findings following puncture implantation under LA (Group A) and (**E**–**H**) open laparotomy under GA (Group B), at two weeks post-modeling. (**A** and **E**) In situ visualization shows tumors located within the liver parenchyma, exhibiting firm consistency (the VX2 tumor is demarcated by the blue dashed circle). (**B** and **F**) Cross-sections of resected tumor specimens reveal elliptical masses with peripheral viable tumor tissue surrounding central necrotic areas. (**C** and **G**) Low-magnification and (**D** and **H**) high-magnification views of VX2 tumor tissues stained with H&E.

characteristic features of squamous cell carcinoma, including significant cellular atypia, readily identifiable mitotic figures, and invasive growth patterns (Figure 4). These results indicate that the tumors obtained by both modeling methods share consistent core biological characteristics.

Discussion

This study provides the first systematic, randomized comparison specifically evaluating the integration of local anesthesia with ultrasound-guided percutaneous puncture for establishing rabbit VX2 liver tumor models. While previous work has validated the percutaneous approach itself,[10,11] our findings extend this knowledge by demonstrating that replacing GA with LA confers distinct advantages. These include superior procedural efficiency, enhanced animal welfare by eliminating GA-related stress and recovery, and a significant reduction in iatrogenic tumor dissemination. This refinement optimizes the model by aligning it more closely with the principles of reduction and refinement in animal research.

Operational Efficiency and Animal Welfare Advantages of the Minimally Invasive LA Technique

This study demonstrated that Group A (experimental) exhibited significant superiority over Group B (control) in anesthesia preparation time, operative duration, and intraoperative blood loss. These advantages stem from the intrinsic properties of the minimally invasive LA technique: local anesthesia eliminates the complex induction and recovery processes associated with GA, while ultrasound-guided precise puncture obviates the need for abdominal wall incision and cavity exposure. This substantially simplifies surgical procedures, shortens operation time, and minimizes iatrogenic injury to normal tissues.[14,15] Consequently, it not only reduces intraoperative risks but also directly alleviates surgical stress and postoperative pain in animals, thereby more comprehensively adhering to the "Refinement" principle in animal experimental ethics.[25]

Beyond procedural convenience, the choice of anesthesia may exert profound biological influences. Evidence suggests that general anesthetics can exert complex effects on immune function and the tumor microenvironment.[8] For instance, the volatile anesthetic isoflurane may suppress natural killer (NK) cell activity, potentially promoting tumor metastasis.[26] In contrast, local anesthetics (eg, lidocaine), in addition to their nerve-blocking effects, have been shown to

directly or indirectly inhibit tumor cell migration by modulating the tumor microenvironment.[27] In the present study, the observed trends toward higher complication and mortality rates in the GA group may be partially attributable to the physiological stress and immune suppression induced by general anesthesia. Therefore, the minimally invasive approach under LA not only reduces direct surgical trauma but may also provide a more physiologically stable experimental system with fewer confounding factors for tumor research.

Model Reliability and Equivalence in Tumor Biological Characteristics

The success of model establishment fundamentally depends on its ability to consistently replicate disease biology. This study confirms that despite the fundamentally different implantation routes, no statistically significant differences were observed between the two methods in either tumor implantation success rate (92.9% vs 85.7%) or tumor volume at two weeks post-operation. More importantly, subsequent imaging (ultrasonography, CE-CT, DSA) and pathological examinations consistently demonstrated that tumors developed by both methods were highly similar in key characteristics, including morphological structure, vascular supply pattern (hypervascular), and histological type (squamous cell carcinoma). This finding is crucial, as it clarifies that despite its less direct implantation route, the minimally invasive puncture technique fully preserves the VX2 tumor's capacity for aggressive intrahepatic growth and its ability to mimic hallmark features of human hepatocellular carcinoma.[2,22] Consequently, models established using the minimally invasive technique are equivalent in reliability to the conventional method and are fully suitable for subsequent interventional therapy, imaging evaluation, and pharmacodynamic studies.

Marked Improvement in Complication Control and Its Scientific Value

The significant reduction in complications represents a major advantage of the minimally invasive LA technique. Although the difference in postoperative infection rates did not reach statistical significance (0% vs 28.6%, $P = 0.102$), the absolute absence of infections in Group A holds clear clinical relevance. More importantly, the significant reduction in peritoneal seeding and abdominal wall invasion observed in the LA group is a major finding. In the open laparotomy group, the mechanical dissemination of tumor cells during liver mobilization, incision, and closure is a plausible mechanism, consistent with the established concept of surgery itself acting as a potential trigger for metastatic spread.[13] In contrast, the percutaneous technique under LA creates a "closed" implantation system, physically isolating tumor tissue from the peritoneal cavity and surgical wound. Furthermore, we cannot rule out a potential pharmacological contribution of lidocaine. Beyond its neural blockade, in vitro and in vivo evidence suggests that local anesthetics like lidocaine may possess anti-migratory and anti-proliferative effects on certain cancer cells, potentially modulating the tumor microenvironment.[27,28] While our study design does not allow us to dissect the mechanical versus pharmacological contributions definitively, the combined approach presents a compelling strategy for minimizing iatrogenic dissemination in preclinical models.

Potential Impact on Interventional Therapy and Translational Research

The minimally invasive LA model established in this study aligns closely with current trends in interventional radiology and precision medicine. In recent years, numerous novel local therapies, such as percutaneous implantation of drug-loaded nanoparticles combined with magnetic hyperthermia,[29] injectable ionic liquid ablation,[7] and the evaluation of novel embolic materials,[17,30,31] rely fundamentally on precise image-guided puncture rather than open surgery. Our modelling approach is conceptually and technically homologous with these advanced therapies, providing a seamlessly compatible and minimally confounding platform for their preclinical evaluation. Furthermore, the LA-based model is particularly suitable for complex experimental designs requiring repeated interventional procedures, such as sequential TACE combined with immunotherapy,[32,33] as it avoids the cumulative risks of multiple general anesthesia episodes and potential immunomodulatory effects, thereby promising broader utility in future translational research.

Limitations and Future Directions

This study has several limitations. First, the relatively small sample size may have limited the statistical power for detecting differences in certain complications, such as infection rates. Second, the observation period was confined to two weeks post-operation, precluding assessment of potential long-term differences in tumor progression and distant

metastasis between the two modelling approaches. Future studies should therefore employ larger cohorts and extended observation periods to further validate our findings. Third, our assessment of animal welfare and pain, while based on objective clinical outcomes (recovery time, activity, feeding, complications), did not employ a standardized, validated behavioral scoring system (eg, the Rabbit Grimace Scale). The incorporation of such refined ethological tools in future studies would provide an even more sensitive and nuanced evaluation of the welfare benefits associated with different modeling techniques. Additionally, integrating multi-omics analyses, such as transcriptome sequencing and single-cell RNA sequencing, to compare the molecular profiles of the tumor microenvironment in both models could provide mechanistic validation of their biological equivalence and elucidate the potential regulatory effects of anesthesia and surgical techniques on the tumor-immune microenvironment.

At last, it is important to acknowledge the inherent limitations of the VX2 tumor model in translational research for HCC. The VX2 line is a squamous cell carcinoma, not a tumor of hepatocellular origin. Its widespread use in liver cancer research is primarily justified by its hypervascular nature, rapid and reliable growth in the liver parenchyma, and its excellent suitability for imaging and interventional radiology procedures, which effectively mimic the vascular and technical challenges of human HCC management.[2–4] However, conclusions regarding HCC-specific tumor biology, molecular pathways, or responses to targeted systemic therapies drawn solely from the VX2 model must be made with caution. This model is most appropriate and valuable for studies focused on the efficacy, pharmacokinetics, and technical optimization of locoregional therapies (eg, TACE, ablation, embolization), imaging modality validation, and investigation of vascular-targeted agents.

Conclusion

In summary, this study demonstrates that ultrasound-guided percutaneous puncture under LA represents a superior strategy for establishing rabbit VX2 liver tumor models. This technique successfully integrates minimal invasiveness, high efficiency, and enhanced animal welfare, as evidenced by significantly shortened anesthesia and operation times, minimal intraoperative bleeding, and reduced physical trauma. Crucially, it maintains key scientific metrics, achieving model success rates and preserving tumor biological fidelity equivalent to those of traditional open laparotomy, while substantially reducing iatrogenic complications such as peritoneal seeding and abdominal wall metastasis caused by surgical manipulation. We therefore recommend this method as the preferred choice for establishing VX2 models. Its integrated advantages in experimental efficiency, ethical compliance, and reliable research background will substantially improve the accuracy and translational value of subsequent preclinical studies in interventional oncology and therapeutic development.

Acknowledgments

We thank Dr. Li Liu (School of Foreign Languages, Southwest Medical University) for her English language editing assistance.

Funding

This work was supported by Luzhou Science and Technology Plan Project (2022-JYJ-153), Sichuan Medical Association Youth Innovation Project (Q2024039), Southwest Medical University Natural Science Youth Project (2022QN114), and Sichuan Provincial Science and Central Guidance Local Exploration Fund Project (2024ZYD0103).

Disclosure

The author(s) report no conflicts of interest in this work.

References

1. Hwang SY, Danpanichkul P, Agopian V, et al. Hepatocellular carcinoma: updates on epidemiology, surveillance, diagnosis and treatment. *Clin Mol Hepatol*. 2025;31:S228–S254. doi:10.3350/cmh.2024.0824
2. Yu H, Zheng S, Wang C, et al. Novel anti-VEGFR2 antibody-conjugated nanobubbles for targeted ultrasound molecular imaging in a rabbit VX2 hepatic tumor model. *J Mater Chem B*. 2023;11:10956–10966. doi:10.1039/D3TB01718D
3. Wu K, Ma S, Xu X, et al. Celecoxib and cisplatin dual-loaded microspheres synergistically enhance transarterial chemoembolization effect of hepatocellular carcinoma. *Mater Today Bio*. 2024;24:100927. doi:10.1016/j.mtbio.2023.100927

4. Gaba RC, Khabbaz RC, Muchiri RN, et al. Conventional versus drug-eluting embolic transarterial chemoembolization with doxorubicin: comparative drug delivery, pharmacokinetics, and treatment response in a rabbit VX2 tumor model. *Drug Deliv Transl Res*. 2022;12:1105–1117. doi:10.1021/acsnano.4c00047
5. Ma Y, Li Z, Luo Y, et al. Biodegradable microembolics with nanografted polyanions enable high-efficiency drug loading and sustained deep-tumor drug penetration for locoregional chemoembolization treatment. *ACS Nano*. 2024;18:18211–18229.
6. Li Q, Liu Y, Guo X, et al. Tirapazamine-loaded CalliSpheres microspheres enhance synergy between tirapazamine and embolization against liver cancer in an animal model. *Biomed Pharmacother*. 2022;151:113123. doi:10.1016/j.biopha.2022.113123
7. Albadawi H, Zhang Z, Altun I, et al. Percutaneous liquid ablation agent for tumor treatment and drug delivery. *Sci Trans Med*. 2021;13:eabe3889. doi:10.1126/scitranslmed.abe3889
8. Xu J, Zhang L, Li N, et al. Etomidate elicits anti-tumor capacity by disrupting the JAK2/STAT3 signaling pathway in hepatocellular carcinoma. *Cancer Lett*. 2023;552:215970. doi:10.1016/j.canlet.2022.215970
9. Li B, Feng G, Feng L, et al. Establishment of a rabbit liver metastasis model by percutaneous puncture of the spleen and implantation of the VX2 tumor strain under CT guidance. *Sci Rep*. 2023;13:2802. doi:10.1038/s41598-022-26706-w
10. Lee KH, Liapi E, Buijs M, et al. Percutaneous US-guided implantation of Vx-2 carcinoma into rabbit liver: a comparison with open surgical method. *J Surg Res*. 2009;155:94–99. doi:10.1016/j.jss.2008.08.036
11. Liu J, Li Y, Zhang J, et al. Comparison of anesthesia and tumor implantation methods for establishing rabbit VX2 hepatocarcinoma. *Am J Transl Res*. 2019;11:7157–7165.
12. Chen Z, Kang Z, Xiao EH, et al. Comparison of two different laparotomy methods for modeling rabbit VX2 hepatocarcinoma. *World J Gastroenterol*. 2015;21:4875–4882. doi:10.3748/wjg.v21.i16.4875
13. Tohme S, Simmons RL, Tsung A. Surgery for cancer: a trigger for metastases. *Cancer Res*. 2017;77:1548–1552. doi:10.1158/0008-5472.CAN-16-1536
14. Meng L, Shan H, He X, et al. Establishment of a modified percutaneous CT-guided paraspinal intramuscular VX-2 squamous cell carcinoma dual tumor model in rabbits. *PeerJ*. 2021;9:e11536. doi:10.7717/peerj.11536
15. Yi HM, Cai BH, Ai X, et al. Establishment of rabbit liver VX2 tumor model using percutaneous puncture inoculation of tumor fragment guided and evaluated by ultrasonography. *Curr Med Sci*. 2019;39:820–824. doi:10.1007/s11596-019-2111-6
16. Feistritzer HJ, Kurz T, Stachel G, et al. Impact of anesthesia strategy and valve type on clinical outcomes after transcatheter aortic valve replacement. *J Am Coll Cardiol*. 2021;77:2204–2215. doi:10.1016/j.jacc.2021.03.007
17. Shi D, Ren Y, Liu Y, et al. Temperature-sensitive nanogels combined with polyphosphate and cisplatin for the enhancement of tumor artery embolization by coagulation activation. *Acta Biomater*. 2024;185:240–253. doi:10.1016/j.actbio.2024.07.022
18. Yuan G, Xu Y, Bai X, et al. Autophagy-targeted calcium phosphate nanoparticles enable transarterial chemoembolization for enhanced cancer therapy. *ACS Appl Mater Interfaces*. 2023;15:11431–11443. doi:10.1021/acsami.2c18267
19. Tian C, Xue X, Chen Y, et al. Phosphotungstate acid doped polyanilines nanorods for in situ NIR-II photothermal therapy of orthotopic hepatocellular carcinoma in rabbit. *Int J Nanomed*. 2022;17:5565–5579. doi:10.2147/IJN.S380370
20. Badwe RA, Parmar V, Nair N, et al. Effect of peritumoral infiltration of local anesthetic before surgery on survival in early breast cancer. *J Clin Oncol*. 2023;41:3318–3328. doi:10.1200/JCO.22.01966
21. Svirskis D, Procter G, Sharma M, et al. A non-opioid analgesic implant for sustained post-operative intraperitoneal delivery of lidocaine, characterized using an ovine model. *Biomaterials*. 2020;263:120409. doi:10.1016/j.biomaterials.2020.120409
22. Yuan G, Xu Y, Wang Y, et al. Development of a Hepatic VX2 carcinoma model in rabbits using an improved minimally invasive method and evaluation with imaging examinations. *J Cancer Res Ther*. 2022;18:1973–1980. doi:10.4103/jcrt.jcrt_1070_22
23. Parvinian A, Casadaban LC, Gaba RC. Development, growth, propagation, and angiographic utilization of the rabbit VX2 model of liver cancer: a pictorial primer and "how to" guide. *Diagn Interv Radiol*. 2014;20:335–340. doi:10.5152/dir.2014.13415
24. Deng G, Zhao DL, Li GC, et al. Combination therapy of transcatheter arterial chemoembolization and arterial administration of antiangiogenesis on VX2 liver tumor. *Cardiovasc Intervent Radiol*. 2011;34:824–832. doi:10.1007/s00270-011-0179-x
25. Lewis DI. Animal experimentation: implementation and application of the 3Rs. *Emerging Top Life Sci*. 2019;3:675–679. doi:10.1042/ETLS20190061
26. Chang C-H, Hwang P-A. Low-molecular-weight fucoidan increases telomere length and immunostimulatory effects on NK-92 cells following inhaled anesthetic injury. *Mutat Res*. 2024;828:111857. doi:10.1016/j.mrfmmm.2024.111857
27. Chida K, Kanazawa H, Kinoshita H, et al. The role of lidocaine in cancer progression and patient survival. *Pharmacol Ther*. 2024;259:108654. doi:10.1016/j.pharmthera.2024.108654
28. Zhang C, Xie C, Lu Y. Local anesthetic lidocaine and cancer: insight into tumor progression and recurrence. *Front Oncol*. 2021;11:669746. doi:10.3389/fonc.2021.669746
29. Xie G, Li B, Guo S, et al. Minimalistic implant for percutaneous magnetic hyperthermia-based combination therapy of hepatocellular carcinoma. *ACS Appl Mater Interfaces*. 2025;17:10369–10379. doi:10.1021/acsami.4c18486
30. Song L, Zhu C, Shi Q, et al. Gelation embolism agents suppress clinical TACE-incited pro-metastatic microenvironment against hepatocellular carcinoma progression. *EBioMedicine*. 2024;109:105436. doi:10.1016/j.ebiom.2024.105436
31. Keum H, Albadawi H, Zhang Z, et al. Bioengineered ionic liquid for catheter-directed tissue ablation, drug delivery, and embolization. *Adv Mater*. 2024;36:e2309412. doi:10.1002/adma.202309412
32. Wang D, Liu J, Li T, et al. A VEGFR targeting peptide-drug conjugate (PDC) suppresses tumor angiogenesis in a TACE model for hepatocellular carcinoma therapy. *Cell Death Discov*. 2022;8:411. doi:10.1038/s41420-022-01198-9
33. Kim H, Choi B, Mouli SK, et al. Preclinical development and validation of translational temperature sensitive iodized oil emulsion mediated transcatheter arterial chemo-immuno-embolization for the treatment of hepatocellular carcinoma. *Adv Healthc Mater*. 2023;12:e2300906. doi:10.1002/adhm.202300906